http://journal.uir.ac.id/index.php/JGEET

E-ISSN : 2541-5794
P-ISSN : 2503-216X

Journal of Geoscience,
Engineering, Environment, and Technology
Vol 8 No 1 2023

RESEARCH ARTICLE

Study of Current Patterns in Tanjung Pasir Banten for Supporting the NCICD SeaWall Development Plan

Reno Arief Rachman[1,2]*, Haryo Dwito Armono[1], Dinar Catur istiyanto[2], Khusnul Setia Wardani[2], Hanah Khoirunnisa[2], Reni Wijayanti[3]

[1] *Departement of Ocean Engineering, Faculty of Marine Technology, Sepuluh Nopember Institute of Technology, Sukolilo, 60116 Surabaya, Indonesia.*
[2] *Research Center for Hydrodynamics Technology, National Research and Innovation Agency, Sukolilo, 60112 Surabaya, Indonesia.*
[3] *Research Centre for Oceanography, National Research and Innovation Agency, Pasir Putih Street, East Ancol 14430, Jakarta, Indonesia*

* Corresponding author : reno001@brin.go.id
Tel.:+6285-22222-333-2; fax:+6285-22222-333-2
Received: Oct 27, 2022; Accepted: Mar 17, 2023.
DOI: 10.25299/jgeet.2023.8.1.10801

Abstract

Hydrodynamic (HD) numerical modeling around Tanjung Pasir waters was carried out using MIKE 21 HD Flexible Mesh software; this modeling was carried out to obtain current pattern conditions (current speed and direction) during the west and east monsoons; this activity was carried out to support NCICD's sea wall construction plan. In addition, the results that will be obtained in this modeling are the conditions of the speed and direction of the current in various tidal conditions during spring and neap. The data used in this modeling include wind speed and direction from European Centre for Medium-range Weather Forecast (ECMWF). Based on the research, the validation value of Naotide tidal data for field tidal data is 93.8%. The HD MIKE 21 surface elevation modeling results on field survey data have a validation value of 93.4%. Extract points 4 and 5 which are the northernmost, have the highest current velocity values compared to the other points. In addition, when conditions are approaching high tide, both spring and neap conditions, the value of the current velocity has the highest value.

Keywords: Sea Wall, Numerical Modelling, Tidal Condition, Current Condition

1. Introduction

The National Capital Integrated Coastal Development Program (NCICD) is part of the National Strategic Program in the 2020-2024 National Medium-Term Development Plan (RPJM). The program is included in the main strategic priority project number 27, the Coastal Security 5 Urban Pantura Java. Conceptually, the NCICD program was implemented to anticipate several prominent issues, such as the threat of flooding, land subsidence, little raw water, and the arrangement of transportation and settlement systems. Several further studies that need to be carried out immediately include a Typical Design study and a study on Detail Engineering Design for the construction of dams, as well as other follow-up studies that can support the implementation of the PTPIN program. One of the following steps is planning to construct an Offshore Reservoir (WLP), which is proposed as a holistic and sustainable solution to the problems faced in Jakarta Bay (Wibowo et al., 2022a). In the WLP concept, it is planned to build an embankment with a length of ± 50.6 km at a depth of -20 m stretching from Muara Cisadane (Banten Province) to Muara Gembong (West Java Province).

The dam will create a reliable flood defense system, storage ponds, and raw water treatment, and also develop coastal areas in Jakarta Bay. The construction is planned to start at the mouth of the Cisadane River as a WLP pilot plant. This development requires planning and study before its implementation to determine the impact and influence of the structural construction. One of the studies needed is a current study in the planned area of the reservoir construction. This study was carried out with numerical modeling to determine the current conditions.

This coastal area is a very dynamic area with various interconnected ecosystems. Changes in the coastline are one form of dynamics of the coastal region that occurs continuously. Shoreline changes that occur in coastal areas are in the form of erosion of coastal bodies (abrasion) and the addition of coastal bodies (sedimentation or accretion) (Suhana, 2015). These processes occur due to the movement of sediments, currents, and waves that interact with the coastal area directly. In addition to these factors, shoreline changes can occur due to anthropogenic factors, such as human activities in the vicinity (Wibowo, 2012).

Important hydrooceanographic parameters include bathymetry, tides, currents, waves, floating sediments, and bottom sediments. Bathymetry is the depth of the sea expressed in depth figures or depth contours measured against a specific vertical datum. The bathymetry condition is temporary because the sea sand extraction location changes continuously. Tides are fluctuations in sea level due to the attraction of objects in the sky, especially the sun and moon, to seawater masses on earth (Gaol et al., 2017). Knowledge of tides (highest and lowest water level elevation) is critical in planning coastal and harbor buildings (Triatmodjo, 2012, 1999). Tides greatly affect human activities living on the coast and are needed for various aspects such as shipping, port layout, pollutant distribution, fisheries development, etc. (Yona et al., 2017). Ocean currents are the movement of seawater transportation. Ocean currents are mainly affected by wind movement and heat differences in the oceans. Ocean currents are more effective as a medium for spreading and diluting pollutants that enter the marine environment (Mukhtasor, 2006). In addition, currents are also strongly influenced by tides. Tidal currents play an essential role as a carrier of nutrients and plankton; they also play an

essential role in diluting and flushing waste that reaches the sea (Mukhtasor, 2006). Floating sediment is all solid substances or particles suspended in water in the form of living (biotic) and inanimate (abiotic) components. Floating sediment is the residue of the total solids retained by a sieve of 2 m or more in size (Lukisworo, 2011). In the west season in the Cisadane River area, the distribution pattern of floating sediment originating from the Cisadane River estuary is very visible; on the contrary, for the east season for the 1-year simulation, the dominant concentration is around 0.12 kg/m3 and the highest is 0.26 km/m3 (Wibowo et al., 2022b).

During pre-reclamation, the current velocity in the southern part of the bay ranged from 0 to 0.94 m/s, while after reclamation, the current velocity decreased to 0 to 0.88 m/s (Aprilia and Pratomo, 2017). One of the reasons for the decrease in the average current velocity after reclamation is the length of the current flow that must be traversed following the shape of the reclamation islands so that the current experiences a decrease in velocity energy (Aprilia, 2017). With the holding of the Reclamation project in Jakarta Bay, the main problem is the decrease in the overall flow velocity in the research area. However, there was an increase in current in several locations around the reclamation island. Procurement of reclamation also causes an increase in the bottom sediment of the waters, leading to an increase in the silting process in the research area.

The hydrodynamic modeling around the thousand islands has been carried out by Khoirunnisa et al. (2021). Based on the modeling results, the validation value between the tidal driver model (TMD) data and MIKE 21 HD is 92 %. Thermal dispersion modeling has also been carried out around the Muara Karang PLTU using three-dimensional MIKE 3 Flow Model Flexible Mesh (Khoirunnisa et al., 2021b). Based on research conducted by Saputra (2018), the current velocity in the master plan condition is smaller than the post-reclamation condition; this is due to the deflection of the current in the reclamation island (Saputra, 2018). Based on the hydrodynamic modeling that has been carried out by Prihantono et al. (2018), during the west season, the longshore currents in Tanjung Pontang dominantly move eastward, while during the east season, some of the longshore currents in Tanjung Pontang move eastward, and some move towards the east and some part move south to Banten Bay (Prihantono et al., 2018).

This study aims to determine the condition of the current pattern around the Cisadane River during the existing conditions using MIKE 21 Flexible Mesh (FM) software for Hydrodynamics (HD) and Spectral wave (SW) modules (Mike 21 DHI, 2017). As input data in this study, secondary data from several source providers and the results of models and field data were used from 30 October to 14 November 2021 (BTIPDP, 2021).

Current modeling and sediment distribution is very important as a step to determine the impact of a natural phenomenon (such as seasonal changes), as well as anthropogenic activities (such as the addition of buildings or land) on the condition of the aquatic environment (Nugraha, 2022).

Until now, studies on currents at the research location planned to build a WLP between the mouth of the Cisadane River and the waters of Tanjung Pasir, Tangerang, Banten (Figure 1) have not been widely carried out. Therefore, a preliminary study of currents in Tanjung Pasir waters was carried out by considering the input discharge value in the Cisadane River. Need an understanding of the dynamics hydrooceanographic conditions in these waters. The dynamics of these waters can be known by recognize the oceanographic parameters of the waters meaning (Kumajas et al., 2007).

Fig 1. Research location around Tanjung Pasir waters, Banten (Google Earth, 2022).

2. Data and Methods

2.1 Material and Data Source

The data used in the current modeling around the Cisadane River are primary data obtained through field surveys conducted on 30 October – 14 November 2021 (BTIPDP, 2021) and secondary data. The primary data used is bathymetric data around the Cisadane River, which results from a field survey (BTIPDP, 2021). The data is then interpolated using the National Bathymetry (BatNas) data with a spatial interval of 180 m x 180 m (BIG, 2021).

Table 1. Material and Data Source

Data	Source and Detail
Bathymetry	Field Survey PRTH-BRIN November 2021 and Batnas v1.5 spacing grid 180 m x 180 m
Wind Data	ECMWF : ERA 5 (Coordinate 5.5 S ; 106.5 E) Time Interval = 3 hours (2021-2022) - (https://cds.climate.copernicus.eu/cdsapp#!/dataset/reanalysis-era5-single-levels?tab=eqc)
Coastline Data	Field Survey PRTH-BRIN November 2021
Tidal	Field Survey PRTH-BRIN November 2021 and Naotide (https://www.miz.nao.ac.jp/staffs/nao99/index_En.htm
Cisadane River Discharge	Term report of Bappenas and ITB 2021

In addition, the surface elevation of the hydrodynamic model was validated against tidal data from the field survey using the Normalization Root Mean Square Deviation (NRMSD) equation. The secondary data used in this HD-SW modeling include data on wind speed and direction, height, and wave period for one year in 2021 with a time interval of 3 hours and a resolution of 0.5 ^{o} x 0.5 ^{o}. In addition, the secondary data used in this modeling is tidal data with a data length of one year extracted through the Naotide model (Padman and Erofeeva, 2005), which has 16 constituents and has been developed by the Japan National Astronomical Observatory (Matsumoto et al., 2000; Miwa and Ikeno, 2008; Saputra, 2018; Sato et al., 2001). Material and data source are presented in table 1.

2.2 Method

2.2.1 Stage of Study

The stages of a research activities start from measurment in the field to modeling of current patterns (Figure 2).

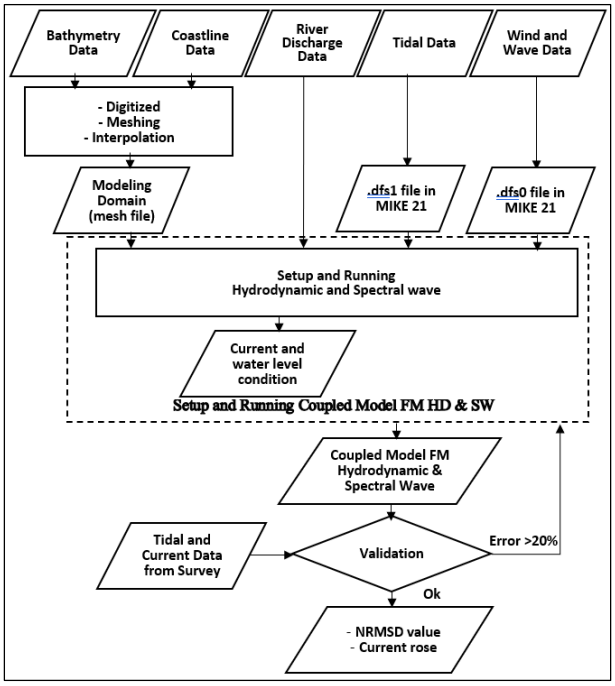

Fig 2. Flowchart of stage activities

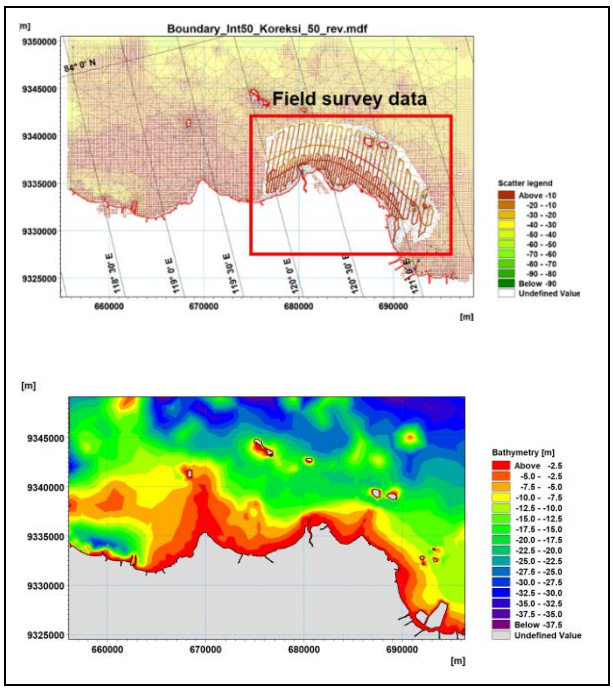

Fig 3. Interpolation results of secondary bathymetry data and field data around Tanjung Pasir waters.

2.2.2 Model Description

The HD – SW modeling uses the DHI MIKE Zero – Mike 21 HD Module, licensed software realease at 2011 from DHI Denmark. Models and methods descriptions are presented in table 2

Table 2. Model and Method Description

Models	Method Description
HD Module from MIKE 21	3645 Flexible Mesh Time simulation from January 1 to December 31, 2021, with a timestep of 300 seconds The number of mesh generated is 10000 mesh with a domain area of 29875 x 44715 m (Figure 3) The essential roughness used in this modeling is 42.3 $m^{1/3}$

Flexible mesh software with a mesh count of 3645 (Mike 21 DHI, 2019). The HD validation modeling was carried out for 20 days from October 30, 2021, to November 19, 2021, with a timestep of 15000 and an interval of 120 seconds. In addition, the essential roughness used in this modeling is 42.3 $m^{1/3}$. The data used in this modeling are wind speed, wind direction from ECMWF (MIke 21 DHI, 2017; Molteni et al., 1996). Other data used in this modeling is data on the average discharge of the Cisadane River and Naotide tides. The next step is to prepare a setup file for hydrodynamic modeling using MIKE 21 software module MIKE 21/3 Integrated Models, Coupled Model FM (.mfm) with modeling time simulation from January 1 to December 31, 2021, with a timestep of 300 seconds (Mike 21 DHI, 2019). Mesh domain modeling for the waters around Tanjung Pasir. In this modeling, the number of mesh generated is 10000 mesh with a domain area of 29875 x 44715 m (Figure 3).

3. Results and Discussion

3.1 Tidal Data Validation

Harmonic analysis of the recorded data is carried out to obtain important water level elevation values such as Highest High Water Level, Mean Higher High Water, Mean Lower High Water, Mean Higher Low Water, Mean Lower Low Water, and Lowest Low Water Level, the results of the analysis are tidal constants tides used in calculating the critical elevations of tides in rivers (Wiguna et al., 2020).

Figure 4 shows a comparison graph between tidal model data and field collection data. Based on the results of this comparison, the error value of each tidal model data on the field data is shown in Table 3., which is 6.2 %, while the most significant error is obtained in the MIKE 21 model data is 12.6 %. Therefore, the tidal model data from Naotide will then be used as input data for HD-SW modeling, both existing and design conditions.

Table 3. NRMSD value between tidal model data and field survey data

No	Sumber	NRSMD (%)
1	*Topex*	7.2
2	TMD	9.2
3	MIKE21	12.6
4	*Naotide*	6.2

Based on Figure 4 (Matsumoto, 2022), the validation between the Naotide tidal model and the 2021 field survey around the mouth of the Cisadane River is 93.8 %. In addition, Figure 5 shows the validation results between the surface elevation values of the MIKE 21 model and field survey data. Based on the figure, the validation value is 93.4 %, and the error is 6.6 %.

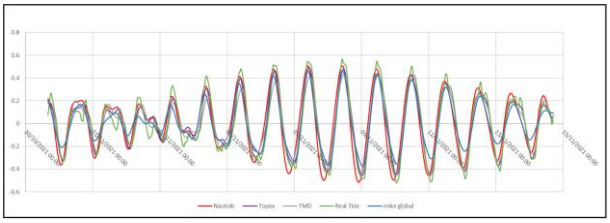

Fig 4. The validation graph between tidal model data (Topex, TMD, MIKE 21, and Naotide) contains field survey data in 2021.

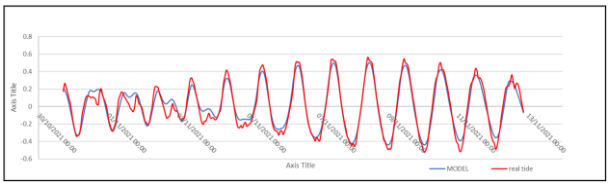

Fig 5. The validation results between the surface elevation values of the MIKE 21 model and field survey data.

3.2 Ocean Current Data Validation

Currents in the river channel are strongly influenced by the ebb and flow of seawater, where when the tide goes upstream and vice versa when it recedes, the current direction goes downstream (Wiguna et al., 2020). Validation of ocean currents data from hydrodynamic modeling with MIKE 21 was also carried out on field ocean currents data. Table 4 shows the current field data collection coordinates around Tanjung Pasir waters.

Table 4. Coordinate points of field flow data collection with ADCP Bottom Mounted

Longitude (E)	Latitude (S)	ADCP
106.631	-5.988	L
106.669	-6.010	UL1
106.668	-6.000	UL2

Figure 6 shows the average value of the current velocity at the ADCP L point based on the results of the MIKE 21 model and field data collection. Figure 7 compares the direction and velocity of the current MIKE 21 HD modeling results with the field results at the ADCP L point. Based on this figure, the difference between the current velocity values from the model results and the field values is 0.03 m/s. In addition, the dominant current direction indicates eastward for both the current velocity of the hydrodynamic model and the results of field data collection.

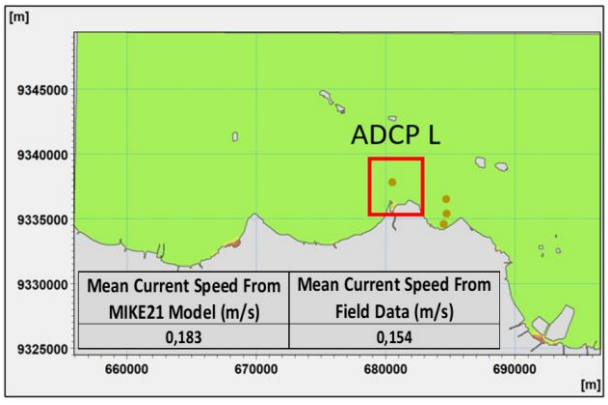

Fig 6. The average value of the current velocity at the ADCP L point based on the results of the MIKE 21 model and field data collection.

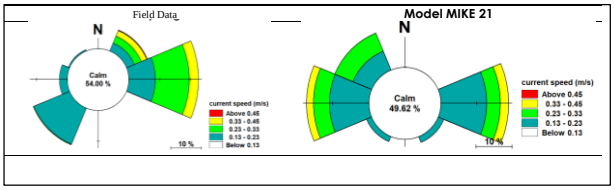

Fig 7. Comparison between current rose from field data collection and MIKE 21 model results.

Figure 8 shows the condition of comparing the speed and direction of the current in a time series between the field data and the data from the MIKE 21 hydrodynamic modeling. In the figure, a black box shows similar conditions between the field data and the data from the MIKE 21 model.

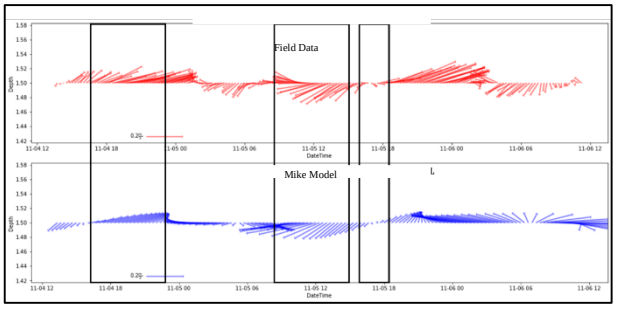

Fig 8. Comparison of the speed and direction of the current at the ADCP L point between the field data and the data from the MIKE 21 model

3.3 Seasonal Conditions of Current Speed and Direction at Each Point

Based on the comparison and calculation of the deviation between the modeling results for one year and NAOTIDE, validation was carried out by calculating the NRMSD (normalized root mean square deviation) value. The sample data calculation was carried out at the northern point of the WLP (-5.9596 North Latitude and 106.59 East Longitude), and the NRMSD value was 0.26 %. Figure 9 is a surface elevation overlay image from MIKE 21 HD modeling with NAOTIDE in June 2021 (1-month sample).

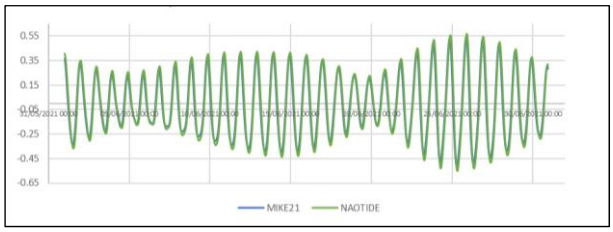

Fig 9. Overlay results between the surface elevation of the MIKE 21 model and the tides of NAOTIDE 1 Month (1 June 2021-30 June 2021)

Figure 10 below shows the location of the modeling carried out, which is around the waters of Tanjung Pasir, Banten, with a small point of tidal data collection for one month (1 - 30 November 2021) depicted as the location of the Tanjung Pasir TPI. The following is the location of the Tanjung Pasir TPI 684801.00 m E, 9334365.00 m (UTM zone 48S). In addition, the figure also illustrates the area of the hydrodynamic modeling along with the points that will be the focus of data extraction. Among them are 5 points, namely the ADCP point, the estuary point, the north point of the WLP, the west point of the WLP, and the top east point of the WLP, with location details contained in the description of Table 5.

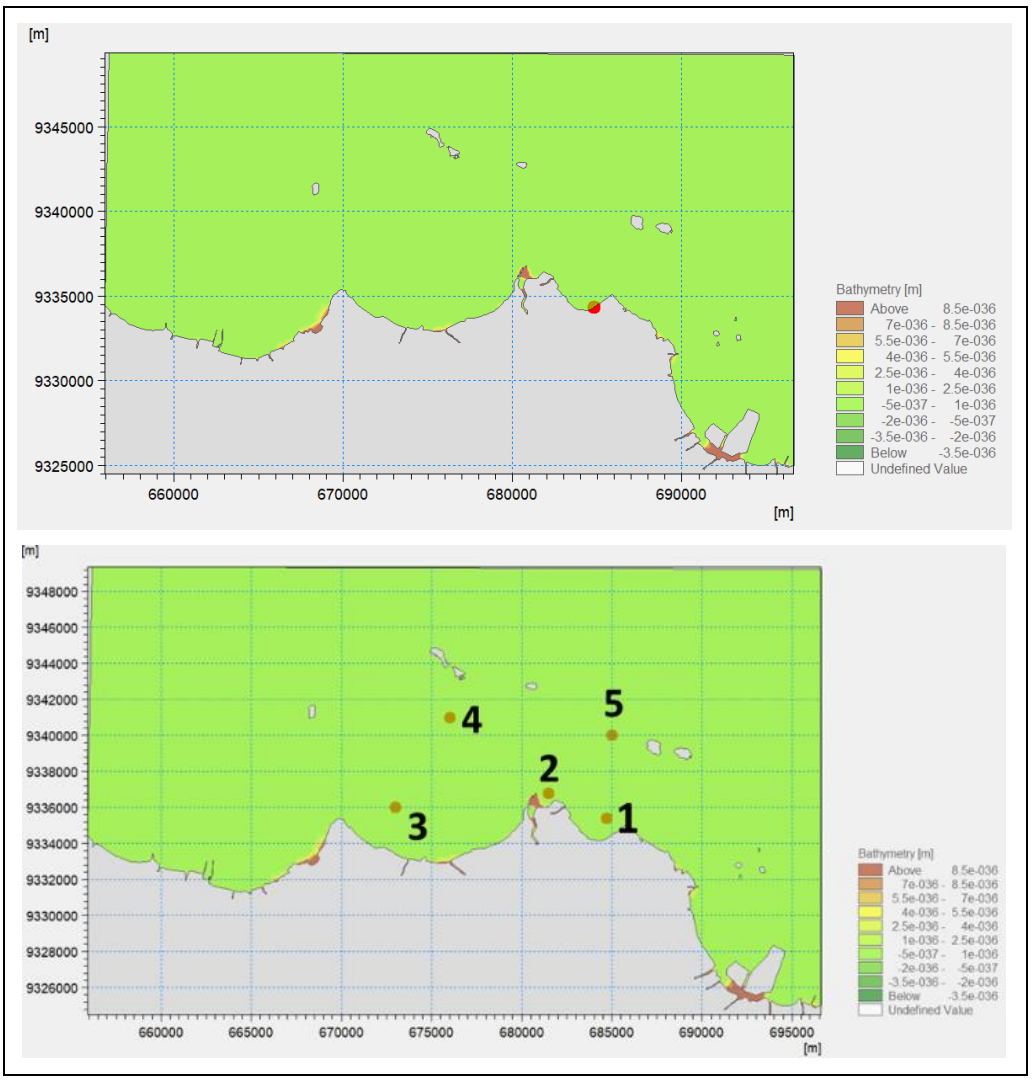

Fig 10. Location of tidal field data collection at TPI Tanjung Pasir station (above) and Location of extract points for analysis of hydrodynamic modeling and spectral wave existing scenarios (bottom)

Table 5. Extract point location in Muara Cisadane existing scenario

Point	Easting	Northing	Information
1	684717.96	9335407.97	ADCP
2	681500	9336800	Estuary
3	673000	9336000	Western WLP 2022
4	676000	9341000	Northern WLP 2022
5	685000	9340000	North Eastern WLP 2022

3.4 Analysis of The Direction And Magnitude Of Currents In The West And East Monsoons

One of the outputs of hydrodynamic modeling is current velocity. This study will analyze the current speed seasonally, namely the west and east monsoons at each observation point (Nugraha, 2022). Based on Figures 11 and 12 below, it can be seen the tidal pattern that occurred for one year around the Cisadane estuary. The following is a flowing plot from hydrodynamic modeling, sampled during the west and east monsoons at the five observation points.

3.4.1 Point 1 ADCP

At point 1 or at the ADCP point location, it can be seen from Figure 11 that in the western season (January-February 2021), the dominant surface current moves eastward, while in the east season (June-August 2021), the predominant surface current moves westward. Then the velocity distribution in the west season is dominated by currents with a magnitude of 0.10-0.20 m/s of 63.3 %, while in the east monsoon is dominated by currents with a volume of 0.00-0.10 m/s of 58.2 %.

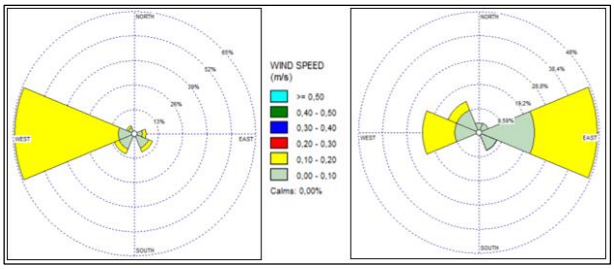

Fig 11. The velocity of the west monsoon (Left) and east monsoon (Right) at point 1 (ADCP)

3.4.2 Point 2 Estuary

At point 2, or a location near the estuary, it can be seen from Figure 12 that the surface currents are equally present in the western season (January-February 2021) and the eastern season (June-August 2021), dominant moving to the northwest. Then for the distribution of the velocity in the west monsoon, it is dominated by currents with a magnitude of 0.10-0.20 m/s of

70.5 %, while in the east monsoon, it is dominated by currents with a volume of 0.00-0.10 m/s of 58.4 %.

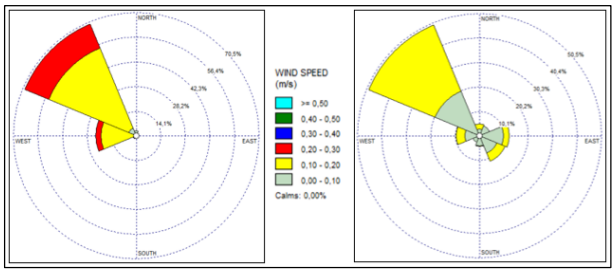

Fig 12. The velocity of the west monsoon (Left) and east monsoon (Right) at point 2 (Estuary)

3.4.3 Point 3 Western WLP

At point 3, or at the western location of the WLP, it can be seen from Figure 13 that in the west monsoon (January-February 2021) and the east monsoon (June-August 2021), the surface currents are equally dominant moving to the northwest. Then the velocity distribution in the west season is dominated by currents with a magnitude of 0.10-0.20 m/s of 65.3 %, while in the east monsoon is dominated by currents with a volume of 0.10-0.20 m/s of 61.3 %.

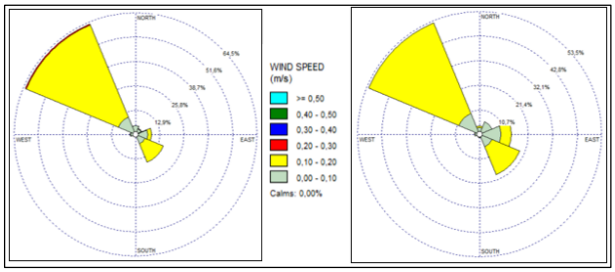

Fig 13. The velocity of the west monsoon (Left) and east monsoon (Right) at point 3 (Western WLP)

3.4.4 Point 4 Northern WLP

At point 4, or the northern location of the WLP, it can be seen from figure 14 that in the west monsoon (January-February 2021) and the east monsoon (June-August 2021), the surface currents are equally dominant moving to the northwest and slightly to the southeast. . Then for the distribution of the velocity in the west season is dominated by currents with a magnitude of 0.10-0.20 m/s of 46.6 % while in the east monsoon is dominated by currents with a volume of 0.10-0.20 m/s of 44.3 %. At the north point of the WLP, both in the west and east monsoons, the currents are more significant than at points 1, 2, and 3. This is because the north point of the WLP is directly adjacent to the high seas, thus affecting the value of a more significant current velocity.

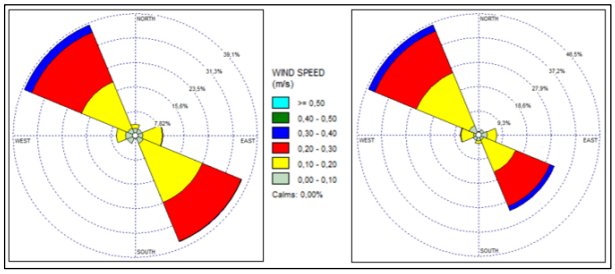

Fig 14. The velocity of the west monsoon (Left) and east monsoon (Right) at point 4 (Northern WLP)

3.4.5 Point 5 North Eastern WLP

At point 5 or in the upper eastern location of the WLP, it can be seen from Figure 15 that in the west monsoon (January-February 2021), the dominant surface current moves to the northwest, while in the east monsoon (June-August 2021), the predominant character current activities to the southeast. . Only at this point 5, the pattern of the dominant current direction is seen according to the influence of the wind direction. When the west monsoon moves from Asia to Australia, the current also moves to the southeast. While in the east monsoon, the wind shifts from Australia to Asia, causing the current to move to the southwest. At points 1, 2, and 3, this pattern does not appear to be possible because the location of the point is closer to the mainland and the coastal influence is still dominant; at point 4, the effect of the coastal area has begun to decrease along with its location which is further away from the mainland/estuarine. Then the velocity distribution in the west season is dominated by currents with a magnitude of 0.10-0.20 m/s of 35.6 %, while in the east monsoon is dominated by currents with a volume of 0.10-0.20 m/s of 36.1 %. At the north point of this WLP, in the west and east seasons, the currents are more significant than at points 1, 2, 3, and 4. This is because the north point of the WLP is directly adjacent to the high seas, thus affecting the value of the current velocity, which is more significant.

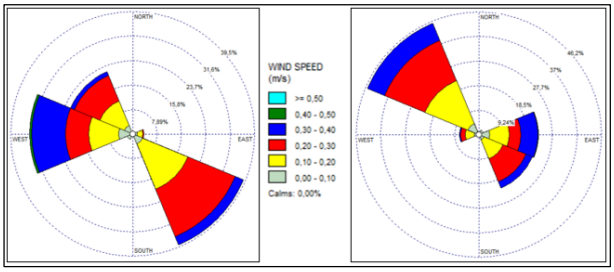

Fig 15. The velocity of the west monsoon (Left) and east monsoon (Right) at point 5 (North Eastern WLP)

3.5 Analysis of Existing Current Velocity and Elevation Conditions in Spring and Neap Conditions

Analysis of surface current velocity conditions was carried out on four conditions, namely at high tide, high tide, low tide, and low tide, respectively, during spring and neap. The following is a sample that will be taken for analysis for these conditions shown in table 6.

Table 6. Extract point location in Muara Cisadane existing scenario

Condition	Spring	Neap
Towards Flood	21-23 Jun 2021	5-8 Mar 2021
Flood	24-26 Jun 2021	9-11 Mar 2021
Towards Ebb	28-30 Jun 2021	12-14 Mar 2021
Ebb	2-3 Jul 2021	15-17 Mar 2021

3.5.1 Towards Flood

Based on Figure 16 above, it can be seen that in conditions leading to high tide according to the data above, in spring conditions, the current dominant moves east to the southeast, while in neap situations, the current dominant moves west to northwest. In spring conditions, statistical results from stations 1 to 5 show the average current is 0.095 m/s with a maximum speed of 0.35 m/s. While in neap conditions, the statistical results from stations 1 to 5 show the average current is 0.09 m/s with a top speed of 0.35 m/s.

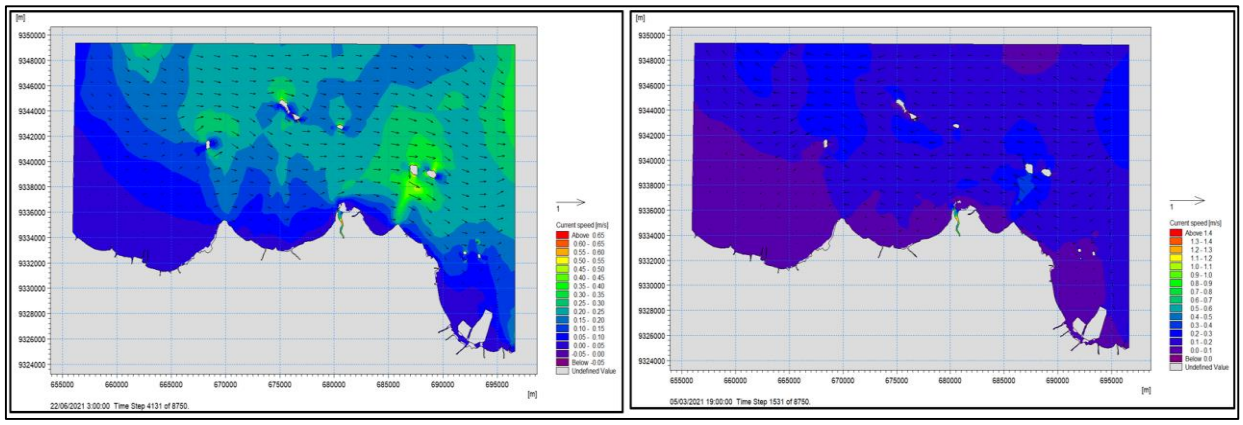

Fig 16. Surface current velocity when toward flood in Spring (Left) and Neap (Right) conditions

3.5.2 Flood

Based on Figure 17, the current dominant moves east to southeast at high tide conditions, according to the sample data above, in spring and neap conditions. In spring conditions, statistical results from stations 1 to 5 show the average current is 0.107 m/s with a maximum speed of 0.37 m/s. While in neap conditions, statistical results from stations 1 to 5 show the average current is 0.87 m/s with a maximum speed of 0.26 m/s.

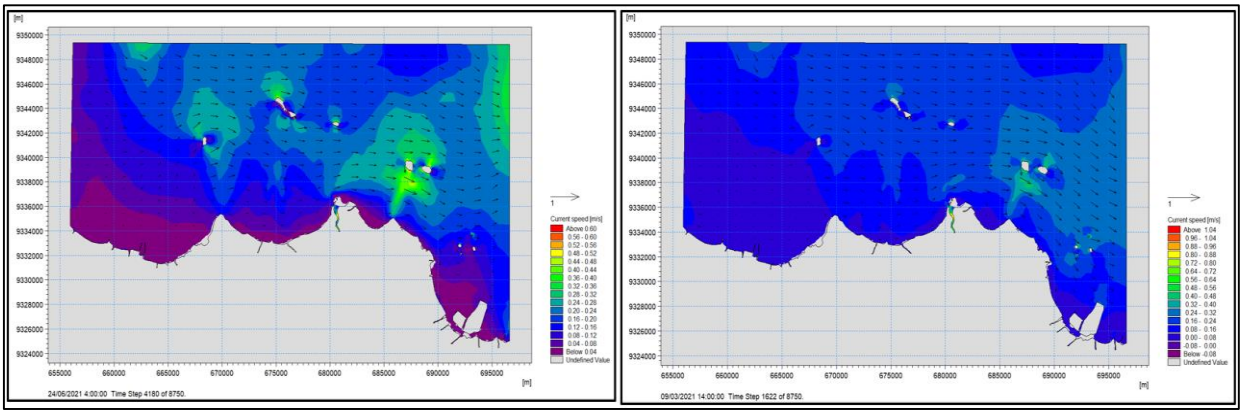

Fig 17. Surface current velocity when flood in Spring (Left) and Neap (Right) conditions

3.5.3 Towards Ebb

Based on Figure 18, it can be seen that at low tide conditions, according to the sample data above, in spring and neap conditions, the dominant current moves northwest to north. In spring conditions, statistical results from stations 1 to 5 show the average current is 0.084 m/s with a maximum speed of 0.33 m/s. While in neap conditions, statistical results from stations 1 to 5 show the average current is 0.071 m/s with a maximum speed of 0.23 m/s.

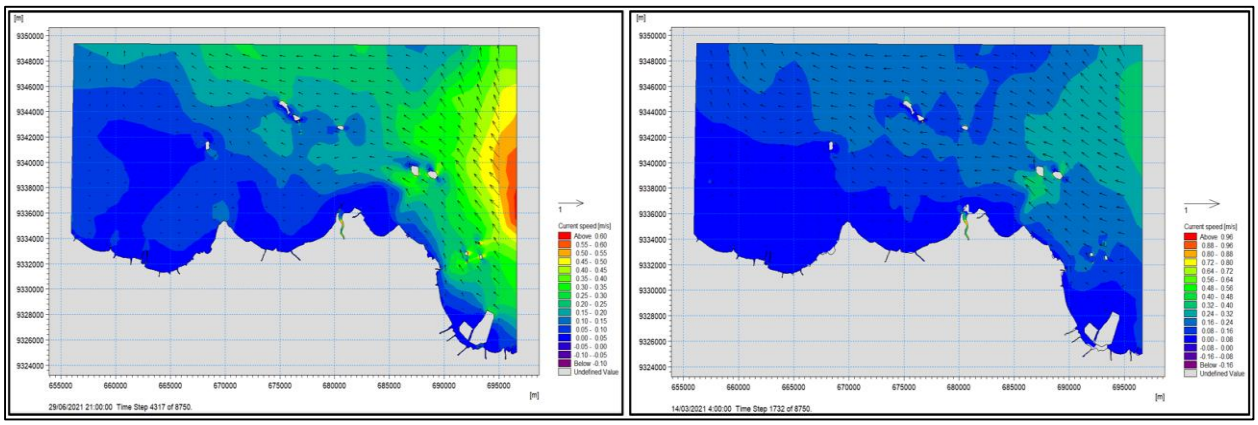

Fig 18. Surface current velocity when toward ebb in Spring (Left) and Neap (Right) conditions

3.5.4 Ebb

Based on Figure 19, it can be seen that at low tide conditions, according to the sample data above, in spring and neap conditions, the dominant current moves northwest to north. In spring conditions, statistical results from stations 1 to 5 show the average current is 0.079 m/s with a maximum speed of 0.26 m/s. While in neap conditions, statistical results from stations 1 to 5 show the average current is 0.071 m/s with a maximum speed of 0.26 m/s.

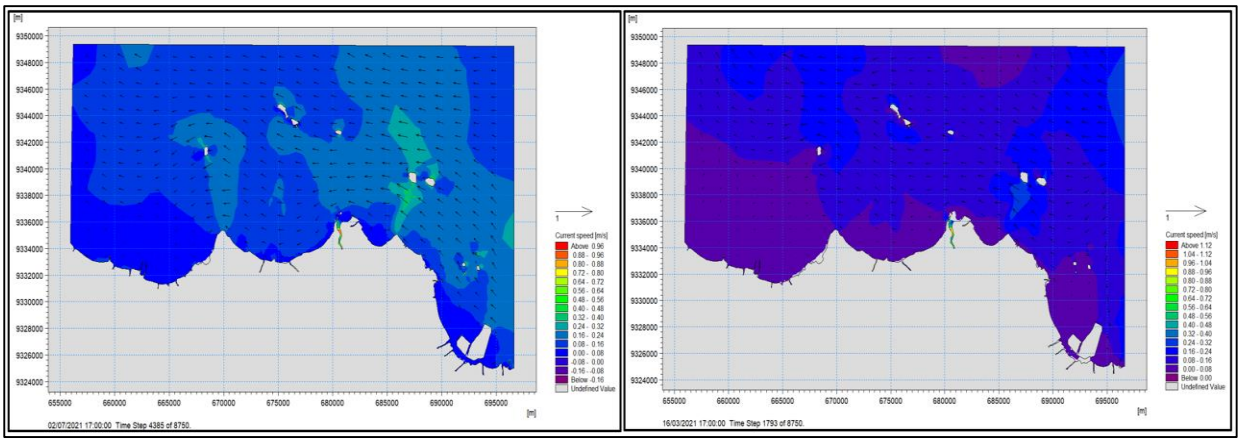

Fig 19. Surface current velocity when ebb in Spring (Left) and Neap (Right) conditions

The results of these statistics can be seen in tables 7 and 8 below:

Table 7. Statistics of Average, Maximum and Minimum Flow Velocity in Spring Conditions From Stations 1,2,3,4,5

Spring	Average Speed (m/s)	Maximum Speed (m/s)
Toward flood	0.095	0.35
Flood	0.107	0.37
Toward Ebb	0.084	0.33
Ebb	0.079	0.26

Table 8. Statistics of Average, Maximum and Minimum Flow Velocity in Neap Conditions From Stations 1,2,3,4,5

Neap	Average Speed (m/s)	Maximum Speed (m/s)
Toward flood	0.09	0.35
Flood	0.088	0.26
Toward Ebb	0.071	0.23
Ebb	0.071	0.27

On the Long Island of the Panjang Islands, east of the waters of Tanjung Pasir, obtained the following results: In the spring conditions, the difference between the highest and lowest current velocities are pretty large (0.018-0.199 m/s); on the other hand when the tides are common in the neap condition (0.008-0.144 m/s), (Khoirunnisa et al., 2021a), these results are almost the same as the results of this study (Tables 7 and 8).

4. Conclusion

The HD MIKE 21 modeling output is the speed and direction of the current in various tidal conditions during spring and neap. The data used in this modeling include wind speed and direction, wave height, wave period, and wave direction. Based on the research that has been done, the validation value of Naotide tidal data on tidal field data is 93.8 %. HD MIKE 21 surface elevation modeling results on field survey data have a validation value of 93.4%. Extract points 4 and 5 which are the northernmost, have the highest current velocity values compared to the other points. In addition, when conditions are approaching high tide, both spring and neap conditions, the value of the current velocity has the highest value.

Acknowledgement

Thank you to the management and staff of the Research Centre for Hydrodynamics Technology- BRIN, especially to members of the PRTH-BRIN Topo-Hydro Survey Laboratory and members of the PRTH-BRIN Coastal Dynamics Numerical Modeling Laboratory, as well as to all project implementers. Assessment and Application of Technology in the Maritime Sector-Innovation of Port Technology and Coastal Dynamics for Fiscal Year 2021. Also, thanks to the Degree by Research (DBR)-BRIN program and the Departement of Ocean Engineering, Faculty of Marine Technology, Sepuluh Nopember Institute of Technology (ITS).

References

Aprilia, E., 2017. 3-Dimensional Hydrodynamic Modeling of Pre and Post-Reclamation Sedimentation Distribution Patterns in Jakarta Bay. Bachelor Thesis. Department of Geomatics Engineering, Faculty of Civil Engineering and Planning, Sepuluh Nopember Institute of Technology.

Aprilia, E., Pratomo, D.G., 2017. 3-Dimensional Hydrodynamic Modeling of Pre- and Post-Reclamation Sedimentation Distribution Patterns in Jakarta Bay Reklamasi Teluk Jakarta. Jurnal Teknik ITS 6, 2337–3520.

BIG, 2021. Seamless Digital Elevation Model (DEM) and BATNAS (Batimetri Nasional) of Tanjung Pasir Waters. Batnas.

BTIPDP, 2021. Bathymetry and Tidal Survey Report of Cisadane Estuary. Agency for the Assessment and Application of Technology. Jogjakarta.

Gaol, A.S.L., Diansyah, G., Purwiyanto, A.I.S., 2017. Analysis of Seawater Quality in the Southern Bangka Strait. Maspari Journal 9, 9–16.

Google Earth, 2022. Google Earth : Maps of Tanjung Pasir Waters, Banten. Google Earth.

Khoirunnisa, H., Wibowo, M., Gumbira, G., Hendriyono, W., Karima, S., 2021a. Numerical Modeling of the Effects of Reclamation and Proposed Infrastructures on Thermal Dispersion of Power Plant Wastewater at PLTGU Muara Karang, Jakarta Bay, in: IOP Conference Series: Earth and Environmental Science. IOP Publishing Ltd. https://doi.org/10.1088/1755-1315/832/1/012043

Khoirunnisa, H., Wibowo, M., Hendriyono, W., Wardani, K.S., 2021b. Hydrodynamic And Boussinesq Wave Modeling for The N219 Amphibious Aircraft Seaplane Dock

Development Plan in Panjang Island. Majalah Ilmiah Pengkajian Industri 15, 87–89.
Kumajas, M., Kumaat, J.C., Moninhkey, A., 2007. Study on Hydro-Oceanographic and Bathymetry conditions of Bajo–Popareng Beach, South Minahasa Regency. Jurnal Geografi dan Pembangunan Wilayah. Manado State University III.
Lukisworo, B., 2011. How to Test Total Suspended Solids (TSS) Gravimetrically, in: Cara Uji Padatan Tersuspensi Total (Total Suspended Solid, TSS) Secara Gravimetri.
Matsumoto, K., 2022. Tidal Prediction System Nao99b. (Accessed Jan 2022). NAO.99b Tidal Prediction System.
Matsumoto, K., Takanezawa, T., Ooe, M., 2000. Ocean Tide Models Developed by Assimilating Topex/Poseidon Altimeter Data into Hydrodynamical Model:A Global Model and a Regional Model around Japan. J Oceanogr 56, 567–581.
Mike 21 DHI, 2019. MIKE 21 Flow Model Hydrodynamic Module User Guide. DHI.
Mike 21 DHI, 2017. MIKE 21 Spectral Waves FM Spectral Wave Module User Guide. DHI.
MIke 21 DHI, 2017. Mike 21 Hydrodynamic Module. DHI.
Miwa, H.;, Ikeno, H., 2008. A Setup Method of Tide Level Variations at Open Boundary in Estuaries for Numerical Tidal Flow Analysis, in: ICHE 2008. Proceedings of the 8th International Conference on Hydro-Science and Engineering.
Molteni, F., Buizza, R., Palmer, T.N., Petroliagis, T., 1996. The ECMWF Ensemble Prediction System: Methodology and Validation. Quarterly Journal of The Royal Meteorologial Society 122 (529), 73–119.
Mukhtasor, 2006. Coastal and Marine Pollution. PT Pradnya Paramita Jalan Bunga 8-8A. Jakarta., Jakarta.
Nugraha, T., 2022. Hydrodynamic Model and Cohesive Sediment Transport in Jakarta Bay Coastal System. Doctoral Dissertation. Institut Pertanian Bogor, Bogor.
Padman, L., Erofeeva, S., 2005. Tide Model Driver (TMD) Manual, in: Tide Model Driver (TMD Manual). Earth and Space Research. https://www.miz.nao.ac.jp/staffs/nao99/index_En.html.
Prihantono, J., Fajrianto, I.A., Kurniadi, Y.N., 2018. Hydrodynamic Modeling and Sediment Transport in Coastal Waters Around Tanjung Pontang, Serang-Banten Regency. Jurnal Kelautan Nasional 1. https://doi.org/10.15578/jkn.v1i2.6614
Saputra, R.A., 2018. Modeling of post-reclamation sedimentation and master plan in Jakarta Bay using Mike21. Doctoral dissertation. Faculty of Science and Technology State Islamic University Sunan Ampel Surabaya.
Sato, T., Hanada, H., Matsumoto, K., Takanezawa, T., Ooe, M.,2001. A Program for the Computation of Oceanic Tidal Loading Effects: "GOTIC" Study of Earth Rotation, Preceission, and Nutation View project Lunar physical libration and navigation View project GOTIC2: A Program for Computation of Oceanic Tidal Loading Effect, Journal of the Geodetic Society of Japan.
Suhana, M.P., 2015. Hydro-Oceanographic Studies for Detection of Coastal Dynamics Processes (Abrasion and Sedimentation). Postgraduate Marine Science, Bogor Agricultural University.
Triatmodjo, B., 2012. Perencanaan Bangunan Pantai, 3rd Edition 2014. ed, Beta Offset. Yogyakarta.
Triatmodjo, B., 1999. Teknik Pantai, 8th Edition 2016. ed. Beta Offset, Yogyakarta.
Wibowo, M., Khoirunnisa, H., Wardhani, K.S., Wijayanti, R., 2022a. Pemodelan Pola Sedimentasi di Muara Cisadane untuk Mendukung Pengembangan Terpadu Pesisir Ibukota Negara. Jurnal Kelautan Tropis 25, 179–190. https://doi.org/10.14710/jkt.v25i2.13732
Wibowo, M., Khoirunnisa, H., Wardhani, K.S., Wijayanti, R., 2022b. Modeling of Sedimentation Patterns in the Cisadane Estuary to Support the Integrated Development of the National Capital Coast. Jurnal Kelautan Tropis 25, 179–190. https://doi.org/10.14710/jkt.v25i2.13732
Wibowo, Y.A., 2012. Dinamika Pantai (Abrasi & Sedimentasi). Faculty of Engineering and Marine Sciences. Hang Tuah University, Surabaya.
Wiguna, E.A., Wibowo, M., Rachman, R.A., Aziz, H., Nugroho, S., 2020. Hydrooceanographic Conditions of the Jelitik River Estuary, Sungailiat, Bangka, Bangka Belitung Province. Buletin Oseanografi Marina 9, 9–18. https://doi.org/10.14710/buloma.v9i1.23363
Yona, D., Sartimbul, A., Iranawati, F., Sambah, A.B., Hidayati, N., Harlyan, L.I., Sari, S.H.J., Fuad, M.A.Z., Rahman, M.A., 2017. Fundamental Oseanografi. UB Press – Universitas Brawijaya University, Malang.

© 2023 Journal of Geoscience, Engineering, Environment and Technology. All rights reserved. This is an open access article distributed under the terms of the CC BY-SA License (http://creativecommons.org/licenses/by-sa/4.0/).